



Automatic detection of symmetry plane for computer-aided surgical simulation in craniomaxillofacial surgery

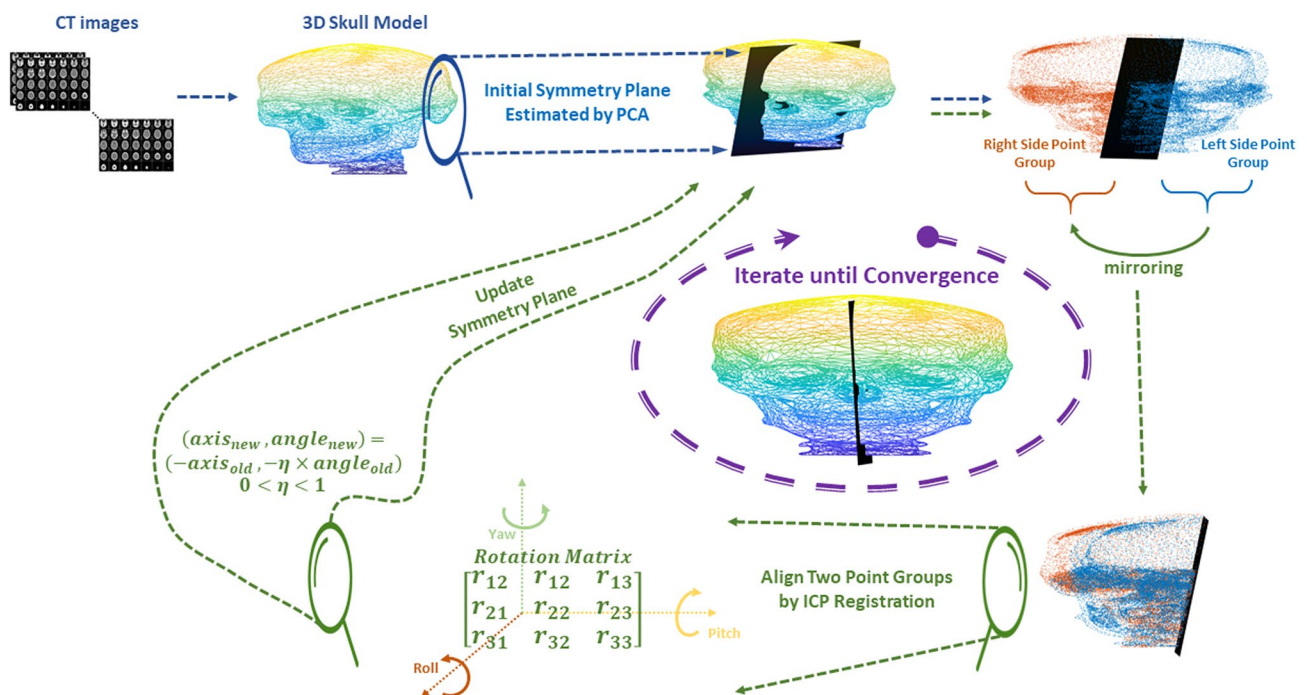
Seyed Mohammad Reza Noori^{1,2} · Parastoo Farnia^{1,2} · Mohammad Bayat^{3,4} · Naghmeh Bahrami^{3,5} · Ali Shakourirad^{6,7} · Alireza Ahmadian^{1,2}

Received: 18 February 2020 / Accepted: 21 July 2020
© Australasian College of Physical Scientists and Engineers in Medicine 2020

Abstract

Symmetry plane calculation is used in fracture reduction or reconstruction in the midface. Estimating a reliable symmetry plane without advanced anatomic knowledge is the most critical challenge. In this work, we developed a new automated method to find the mid-plane in CT images of an intact skull and a skull with a unilateral midface fracture. By use of a 3D point-cloud of a skull, we demonstrate that the proposed algorithm could find a mid-plane that meets clinical criteria. There is no need for advanced anatomical knowledge through the use of this algorithm. The algorithm used principal component analysis to find the initial plane. Then the rotation matrix, derived from an iterative closest point (ICP) registration method, is used to update the normal vector of the plane and find the optimum symmetry plane. A mathematical index, Hausdorff distance (HD), is used to evaluate the similarity of one mid-plane side in comparison to the contralateral side. HD decreased by 66% in the intact skull and 65% in a fractured skull and converged in just six iterations. High convergence speed, low computational load, and high accuracy suggest the use of the algorithm in the planning procedure. This easy-to-use algorithm with its advantages, as mentioned above, could be used as an operator in craniomaxillofacial software.

Graphic abstract



Extended author information available on the last page of the article

Keywords Sagittal plane · Mid-plane · Symmetry plane · Computer-aided surgery · Maxillofacial fracture · Cranio-maxillofacial surgery

Introduction

Accurate symmetric plane restoration plays a crucial role in unilateral fracture reduction and skeletal reconstruction planning [1]. The symmetry plane, also known as the midsagittal plane, is essential for a patient-specific implant design procedure and orthognathic surgery planning [2, 3]. Quantifying the precise symmetry plane is a controversial issue in computer-aided surgical simulation (CASS), as no gold standard exists [3–7]. The symmetry plane that is used in CASS is estimated manually, based on anatomic landmarks. This approach requires advanced anatomical knowledge and is time-consuming. Presently, the development of an automatic method for calculating a symmetry plane remains a challenge [9].

There are two substantial problems. The first is how to estimate the most appropriate symmetry plane to halve the skull evenly, and the second is how to assess the accuracy quantitatively. The ideal symmetry plane divides the skull into two mirror halves. However, a real skull is never truly symmetrical. Depending on the searching strategy, different symmetry planes could be acceptable. Thus, we are seeking the optimum midplane with minimal errors of symmetry; additionally, clinical criteria must be approved.

Several studies investigated these challenges [1–12]. Cevidane et al. quantified the extent of the asymmetry of the mandibular using two different approaches [1]. In the first approach, they found the symmetry plane through manually chosen anatomic landmarks. In the second one, an arbitrary mirrored skull model was registered on the original skull thorough a rigid voxel-based method. The authors reported that the results of the first method are more acceptable than the second. However, the landmarks could be obscured by trauma or disorders such as tumour-removal surgery. Since manual selection of landmarks is not desirable, this method could not be used in many craniomaxillofacial reconstructions. They believed the second method is less subjective and could present acceptable results. The idea of finding the symmetry plane in this research is admirable, but the method suffers from a lack of a reliable validation routine.

Berlin et al. investigated 2D-asymmetry analysis techniques [12]. They categorised symmetry-analysis methods based on different lines and anatomic points on the face image. It is not possible to find the best symmetry plane using 2D data from the facial image individually, especially in prosthesis design procedures. Li et al. suggested a principal component analysis (PCA) based on an adaptive minimum-Euclidean-distance (PAMED) approach to find an

optimal object reference frame for the symmetrical alignment of the dental arch during CASS [3]. They showed that standard PCA is not reliable for symmetry-plane estimation since it is vulnerable to noise and outliers. The proposed method could address the shortcomings of PCA, even for missing teeth. To this end, the Y-axis is defined as perpendicular to the line on the X-axis that connects two corresponding landmarks on the left and right side of the dental arch, e.g. tip of the left and right canines, in the axial plane. Firstly, the PCA is used to find the initial symmetry plane. Then, all points are projected onto the X–Y plane. Now, if the Y-axis moves to the right or left in the X–Y plane, then the symmetry plane (Y–Z plane) is adjusted and deviation of the initial plane is compensated. This is done until the Euclidian distance between a minimum of two side-points is achieved. The PAMED method is designed for symmetrical alignment of the dental arch for orthognathic surgery planning. This method is suitable for the dental arch but could not be generalised for the skull symmetry plane, since manual landmark selection in the skull is not always feasible, as explained previously. Moreover, dimension reduction (Z-axis) in the skull causes loss of beneficial information. Furthermore, by asking three experts to opine, an utterly subjective methodology was used for the evaluation of the symmetry plane. Martini et al. determined the symmetry axis and examined the quantity of asymmetry mathematically in patients with craniosynostosis [10]. Their proposed method was based on 3D-scanned soft-tissue data and the landmark-based 3D analysis. A symmetry axis is defined by anatomical landmark pairs. Then the distance from the landmarks to the line is calculated. The symmetry plane is estimated from the symmetry axis. In order to minimise the perpendicular distance of landmark pairs from the symmetry axis, the symmetry axis algorithm was moved. The particular kind of method conducted in this work was simple and easy to implement, although it was depended on accurate anatomical landmarks. Bockey et al. developed an asymmetry index (AI) [2]. AI is based on the mean distance between the original and the mirrored set. The diagonal of the bounding box of the face is used to normalise faces of different sizes. They used AI retrospectively in patients with orbital defects. AI shown better results when a healthy surface is mirrored on the side of the defect, in comparison with using a digitally computer-aided design template. The analysis was based on 3D facial data recorded optically. Although optical data is exposed to no radiation, there are always some facial areas that remain unrecorded. Additionally, the 3D model from CT images allows us to make a precise observation of different views and to highlight vital structures.

The avoidance of manual landmark selection and symmetry-plane estimation is an ongoing challenge. Another is the objective evaluation of the suggested plane. This research aims to develop an automated method based on an iterative process by minimising the error-index of the symmetry plane. Analytical data processing is performed on 3D point-sets, derived from CT images. Firstly, an initial symmetry plane estimated by the PCA and skull point-set was divided into two groups by the plane. Then, the ICP registration method was used to match two point-sets. Our main contribution was to use the rotation matrix derived from the registration method to correct the initial symmetry plan automatically. Finally, we suggest this technique for finding a symmetry plane in both intact and simple fractured skull cases. Craniomaxillofacial reconstruction and orthognathic surgery planning would be within the scope of our research.

In the following sections, firstly, we describe datasets that are used. Subsequently, we explain the different steps of the proposed algorithm. Then, the results obtained from intact and fractured skull CT datasets are reported. Finally, the discussion is placed.

Materials and methods

Datasets

Computed tomography (CT) images of 15 intact bones were taken from Parseh Intelligent Surgical System Co. datasets, Tehran, Iran. The patients ranged in age from 22 to 59 years with an average age of 34.5 ± 15.32 years. The slice thickness of images was equal to or less than 1 mm. Another set of CT images from seven patients with unilateral midface fractures were taken from the radiology department, Sina Hospital, Tehran University of Medical Science (TUMS), Tehran, Iran. Patients ranged in age from 21 to 56 years, with an average age of 32.71 ± 13.35 years. The slice thickness of images was about 1 mm. All CT image files were in digital-imaging communications in medicine (DICOM) format, obtained from the head and some vertebrae of each individual.

Method

The flowchart of the proposed method is shown in Fig. 1. The procedure starts with the pre-processing section. First of all, CT images were imported into the 3D slicer, open-source software, to analyse and visualise the information derived from medical images [13]. After bone segmentation, the bone data was exported as a stereolithography (STL) file. This file includes vertices and faces to describe the skull information. Vertebrae were omitted. The computations were done using MATLAB 2017b (The MathWorks, Inc,

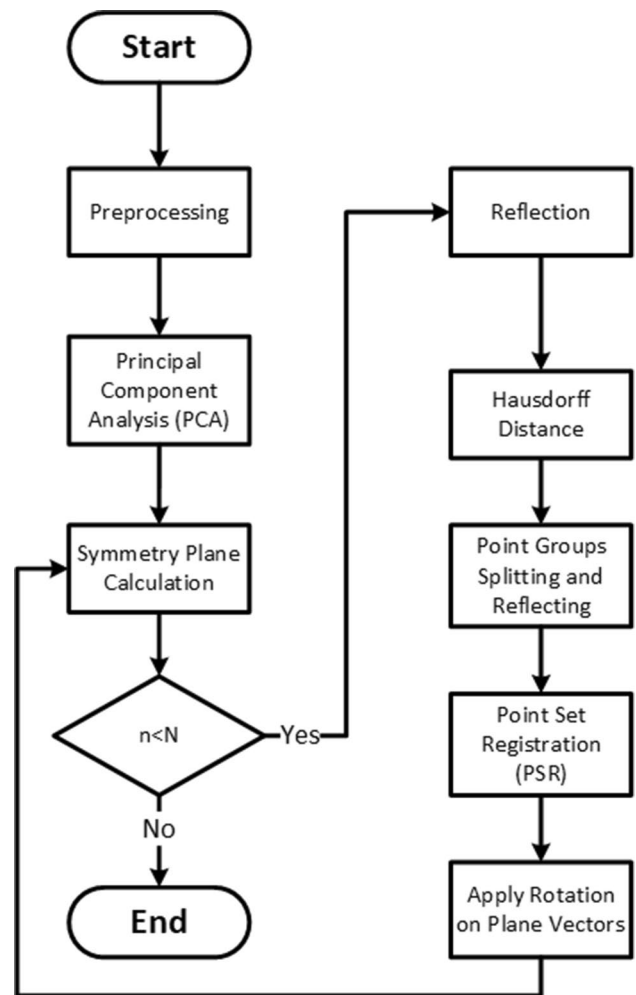


Fig. 1 Flowchart of the proposed method for precise symmetry plane estimation of the skull

Natick, MA) and implemented on a Core i5 CPU, 3.00 GHz with 16 GB Ram.

Principle component analysis (PCA)

PCA is a powerful tool for structural statistical model-analysis in many fields [14]. The central concept and function of PCA is to reduce the dimensionality of a dataset, according to the vectors with the greatest quantity of information (principal components) or variance. Hence, two main outputs that come from PCA are eigenvectors (main directions), and eigenvalues (magnitude of variation).

After pre-processing, PCA is applied to the point-set of 3D data. Therefore, three eigenvalues and eigenvectors are provided. The centre of mass of the skull is calculated by averaging all skull landmark points. Because of the intrinsic properties of the human skull, the plane contained two eigenvectors with larger eigenvalues, and also the centre of

mass of the skull could be an initial estimation for the location of the symmetry plane. Figure 2 shows these data.

The symmetry plane divides data-points into left and right point-groups. Then, the right point-group reflects on the contralateral side through the symmetry plane. The distance between the point-groups on each side determines the error-index of the symmetry plane. The error-index is calculated through Hausdorff Distance (HD). PCA does an excellent job of finding the coarsely-tuned symmetry plane. Then we performed further processes to find the best fine-tuned plane.

Point set registration (PSR)

In the PSR procedure, a spatial transformation is computed in order to match two point-sets. PSR is used in pattern recognition and computer vision for many medical applications, such as compensation of tissue deformation and statistical shape models [15–17]. The PSR process consists of both rigid and non-rigid registration. In rigid registration, transformation terms are translation vector, rotation matrix, and sometimes scaling factor. Transformation of a non-rigid registration contains nonlinear deformations [18].

One of the most popular PSR algorithms is the Iterative Closest Point (ICP) [19, 20]. The central assumption of this algorithm is that the closest point-pairs between source and model point-sets correspond with each other. The conventional ICP algorithm works for rigid transformation problems. The ICP algorithm finds corresponding point-pairs in the model (M) and the source (S) point-set. Then, it computes a transformation matrix in order to minimise the distance of corresponding point-pairs. Error in the ICP algorithm is calculated in the way of point-to-point

measurement. The main minimisation problem is shown below:

$$E(\mathbf{R}, \mathbf{t}) = \sum_{i=1}^{N_M} \sum_{j=1}^{N_S} \omega_{ij} \|m_i - (\mathbf{R}s_j + \mathbf{t})\|^2 \quad (1)$$

where $m_i = (m_{ix}, m_{iy}, m_{iz})^T \in M$ and $s_j = (s_{jx}, s_{jy}, s_{jz})^T \in S$ arrange a correspondence pair, N_M and N_S states the number of points in M and S , respectively, and ω_{ij} are the weights for a pair. In a conventional ICP algorithm, if the pair correspond, $\omega_{ij} = 1$, otherwise $\omega_{ij} = 0$. Also, \mathbf{R} , a 3×3 matrix, and \mathbf{t} , a 3D vector, stand for rotation and translation respectively. Since the ICP algorithm was introduced [19, 20], different variations of the ICP algorithm have been developed based on its fundamental concept [21]. In the following, some effective stages of the ICP algorithm are described.

Subsampling The number of landmark points in each set is an essential parameter for computational complexity. There are various methods to reduce the number of landmarks while preserving crucial information [22]. In these cases, each dataset contains many faces (a triangulate flat surface that connects every three vertices), edges (where two faces meet), and vertices (a corner where edges meet). Vertices are points in 3D space that embody the skull. The number of faces and vertices in the dataset was about 650,000–850,000 and 325,000–425,000, respectively. We define the reduction factor as the detraction of the number of faces so that the number of edges and vertices is decreased. The reduction factor was increased until ICP results were preserved.

Point distance measurement In the conventional ICP, the correspondence of each point is chosen by measuring the

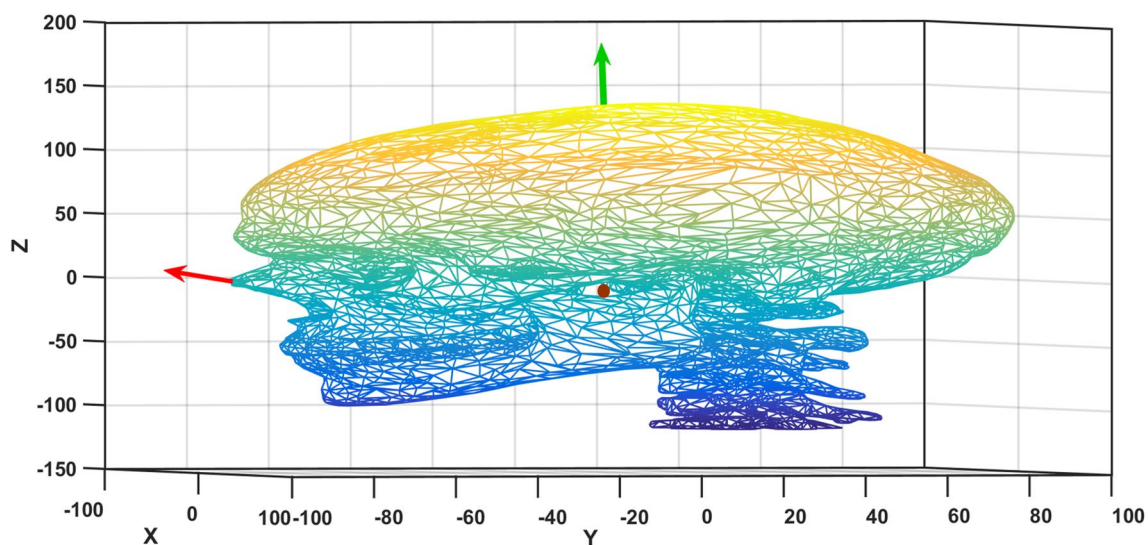


Fig. 2 Point set of an intact skull with two principal eigenvectors (green and red arrow) and centre of mass of data (dark red point)

distance from all other points [19]. Therefore, the computation is too complex and time consuming. The kD-tree method could accelerate the correspondence process. KD-tree stands for a k-Dimension tree, which is a multidimensional binary search tree for storing information that can be retrieved by associative searches [23]. Each leaf node is a k-dimensional point, and each non-leaf node is a dividing plane (in 3D space) that partitions spaces into two segments, named half-spaces. The points placed to the right side of the plane comprise the right subtree of that node, and the points placed to the left side of the plane comprise the left subtree. Each node in the tree is related to one of the k dimensions. The plane direction is perpendicular to the axis of the dimension [23, 24]. Based on these node properties, the tree is constructed.

The kD-tree structure is exploited by the ICP algorithm to find corresponding point-pairs. By using the K-nearest neighbour (KNN) algorithm, it is possible to retrieve the closest data-point to the point to be queried in the kD-tree. KNN queries are regularly applied to multidimensional spaces [25]. They found K closest points to a query-point, based on distance criteria. Here K equals unit, as the closest point of query point is retrieved. In each iteration of the ICP algorithm, when the source is aligned onto the model, the kD-tree structure is applied to the data. Then, the nearest point-pairs are found.

Update symmetry plane

The main idea of our method is to use the rotational angle derived from the rotation matrix to update the symmetry plane. In the first iteration, the symmetry plane contains the centre of mass, and two principal eigenvectors come from PCA. In the next iterations, skull landmarks are divided into left and right point-groups. The left point-group is mirrored to the contralateral side through the plane. Then the right side-point group is considered to be the model and the mirrored left side point-group is considered to be the source. Next, the source data is registered to the model by the ICP algorithm and the rotation matrix is calculated. The rotation matrix is converted to an axis–angle rotation representation through Euler’s rule. Axis–angle representation contains a unit vector indicating the direction of the rotation axis, and an angle stands for the rotation magnitude about the axis. We define a new axis–angle rotation as follows:

$$(axis_{i+1}, angle_{i+1}) = (-axis_i, -\eta \times angle_i); 0 < \eta < 1 \quad (2)$$

where $axis_i$ and $angle_i$ show direction and magnitude of the rotation axis in i th iteration, respectively. η is a convergence coefficient. We used $\eta=0.9$, obtained heuristically. A negative sign is used since we want to compensate for the amount

of rotation between the two groups. After reconversion of the new axis–angle rotation to a rotation matrix, the orientation of eigenvalues can be updated as follows:

$$Ev_{i+1} = Ev_i \times R_{i+1}^T \quad (3)$$

where Ev_i and R_i^T are eigenvector and transposition of the rotation matrix of i th iteration, respectively. As Fig. 1 shows, a new symmetry plane is calculated by newly adjusted eigenvectors. Applying this idea results in a significant reduction in point-set registration errors in the next iteration. We assumed that in the ideal skull, the symmetry plane always contains the centre of mass point. Hence, after initialising the symmetry plane, only the rotation matrix is needed in order to fine-tune the plane. Therefore, there is no need to use the translate vector from the ICP in the tuning procedure.

Symmetry plane evaluation

Accuracy quantification of the estimated symmetry plane could be done with a variety of mathematical distance measures. It is assumed that an ideal symmetry plane splits the skull into two similar point-groups. Then two point-groups could be matched optimally by reflecting one group in the symmetry plane. The distance between the reflected point-group and the other one could be a useful error index. One-sided HD is one of the most reliable measures of symmetry between two point-groups and is used widely in computational geometry [26]. Ghadimi et al. developed a segmentation method from CT images of newborn babies [27]. They used the HD method to compare manually segmented images with the images segmented by their segmentation method. One-sided HD (d_{HD}) is calculated as follows:

$$d_{HD}(A,B) = \max_{a \in A} (\min_{b \in B} \|a - b\|) \quad (4)$$

where A and B are two point groups, and $\|\cdot\|$ is the Euclidean distance.

In the proposed method, the number of iterations, N , is the stopping criteria. N is chosen to be 10, empirically.

Results

To evaluate the ICP algorithm method, we used 15 datasets from intact skulls. In order to know the optimum factor of data sampling, different reduction factors, r , were evaluated heuristically. The HD is plotted for different r in Fig. 3. The ICP algorithm was run for 100 iterations.

Since the algorithm converged after six iterations, the time consumed by the ICP algorithm in the sixth iteration was recorded for different r in Table 1. The ICP time consumption slumped when the r reduced. From Fig. 3 and Table 1 it can be concluded that if $r=0.075$, the

Fig. 3 Comparison of the effect of different reduction factors (r) on the Hausdorff distance (HD) values in each iteration. This is for a single subject

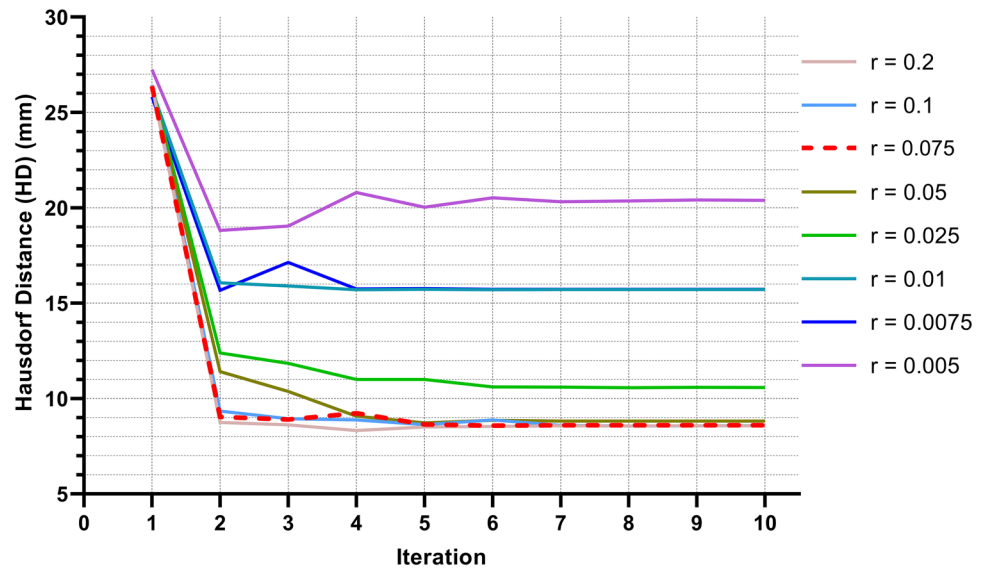


Table 1 ICP registration time consumption vs. reduction factor (r)

Reduction factor (r)	ICP time (s)
0.2	2124
0.1	445
0.075	280
0.050	135
0.025	40
0.01	6

The best r value is shown in the bold

Table 2 Run times and HD values in the conventional and proposed ICP algorithms for five intact skulls

Data #	Conventional ICP		Proposed ICP		Vertices # ($r=0.075$)
	Run time (s)	HD (mm)	Run time (s)	HD (mm)	
280.14	8.57	2.75	8.57	30,583	
191.45	7.50	2.11	7.50	22,413	
270.60	6.81	2.80	6.81	30,240	
258.31	6.50	2.42	6.50	29,705	
220.63	7.32	2.26	7.32	24,985	

best results concerning HD and time losses conducted are achieved. The elapsed CPU time used by the overall algorithm for $r=0.2$ and $r=0.075$ is 78,350 and 10,590, respectively.

Instead of the conventional ICP algorithm, we ran the algorithm with kD-tree, $r=0.075$, and compared the ICP performance in the sixth iteration. The run-time was reduced by about 99 times. The run-time and HD of five intact skulls were inserted into Table 2. We improved the conventional

ICP algorithm by use of kD-tree and named it *proposed ICP algorithm*. A comparison between run-time and HD in the conventional and proposed ICP algorithms is shown in Table 2.

Visualisation of each iteration for one skull is complete. Figure 4 shows how an initial symmetry plane adjusts through iterations to reduce HD. In Fig. 4a and b, X–Y and X–Z views are captured, respectively. Figure 5a indicates how the symmetry plane halves skull data in each iteration (X–Y view). Figure 5b visualises the right side of the skull and the mirror of the contralateral side in the X–Y view. Figure 6 demonstrates how the calculated symmetry plane halves data in axial, coronal, and 3D views. It is notable that the first plot of Figs. 4, 5, 6 and 7 implies an initial symmetry plane calculated by PCA, and the others are updated versions calculated by the ICP algorithm.

We applied the proposed algorithm on seven datasets from patients with midface fractures. The results were similar to the intact-skull data, and the initial HD decreased around 65% after six iterations. Figure 7 demonstrates how the calculated symmetry plane halves data in axial, coronal, and 3D views for a fractured zygomatic arch. We show the rotational-angle variations in different iterations for intact and fractured skulls in Fig. 8. For a comparison of HD values in intact and fractured skull data, the results are plotted in Fig. 9.

Discussion

Defining a symmetry plane is the key to apply the mirroring technique in CASS. There is no gold-standard, non-subjective method to estimate a symmetry plane. In this study, we propose a reliable, objective method for symmetry-plane calculation, which requires no explicit anatomical knowledge.

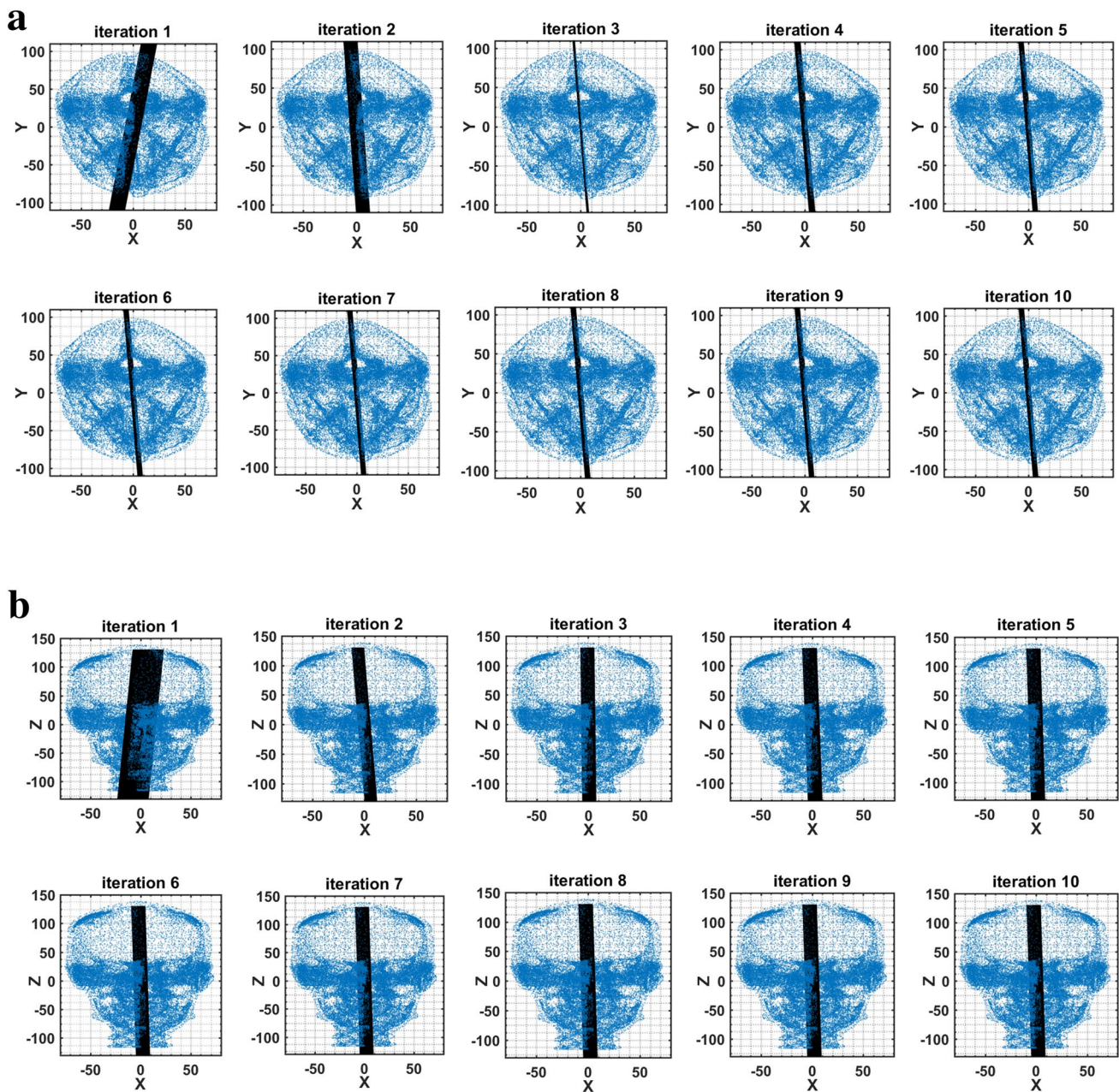


Fig. 4 The estimated symmetry plane in each iteration reduces Hausdorff distance (HD) as an error index. **a** X–Y view is captured. **b** X–Z view is captured

Since the proposed algorithm finds the symmetry plane in an unsupervised way, by simply importing proper pre-processed data, we named it an *automatic* algorithm.

The main contribution of this research is applying rotations to the initially-captured PCA symmetry plane. First,

the centre of mass point of skull landmarks is calculated. PCA is applied to the landmarks and eigenvectors are calculated. So, the initial plane is estimated using the centre of mass and two main eigenvectors. Then, landmarks are divided into left and right point-groups, based on the

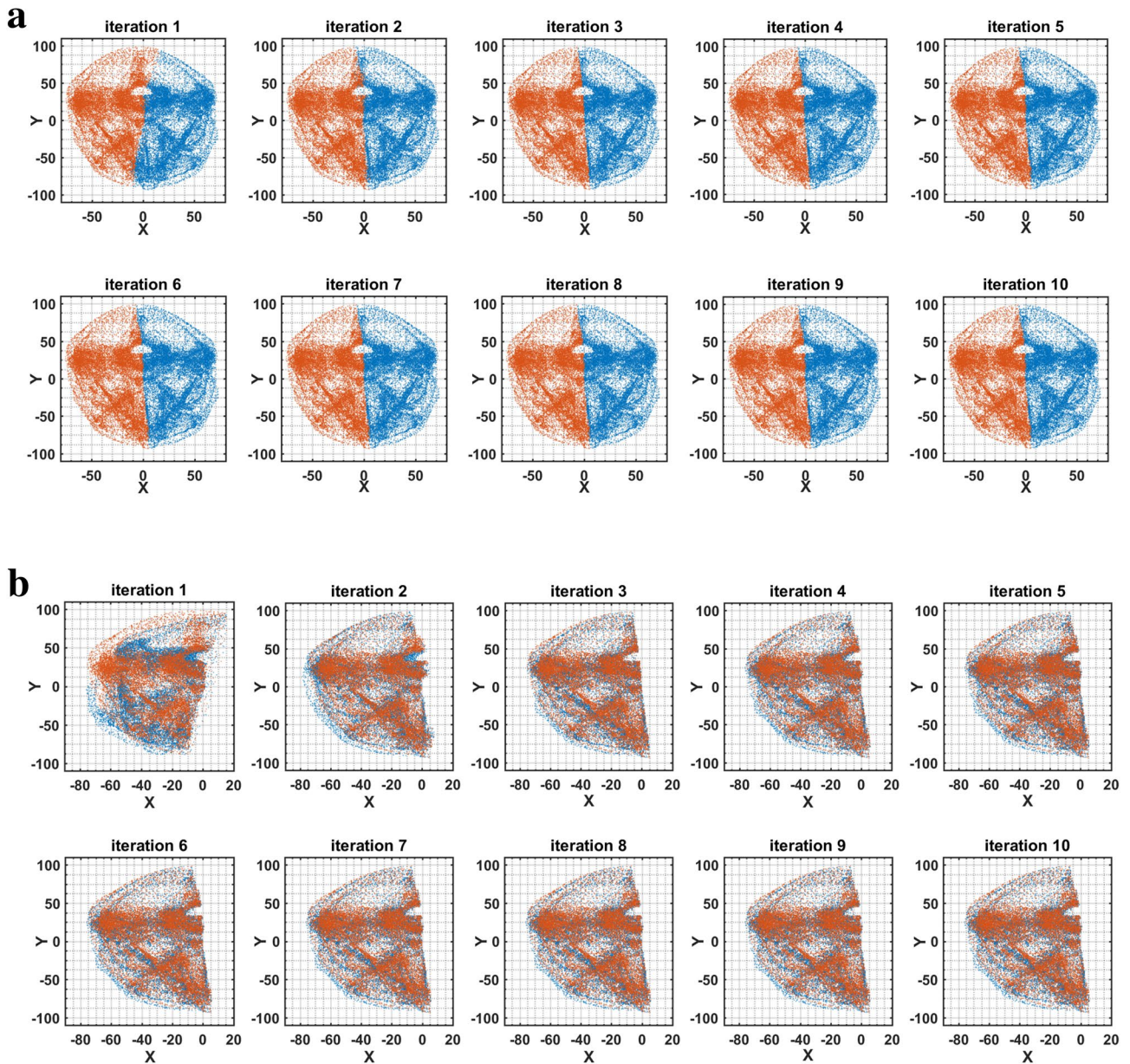


Fig. 5 Visualisation of updates in the symmetry plane. **a** Data split into two different point-groups that are on the left and right side of the symmetry plane, in each iteration (X–Y view is captured); **b** right

side point group reflected through symmetry plane, in each iteration (X–Y view is captured)

plane. The left point-group is mirrored to the contralateral side through the plane. Then, the ICP rigid-registration algorithm is used to align point-groups accurately. The rotation matrix from the ICP algorithm is used to derive rotation axis and angle. Then, the rotational angle is

applied to the eigenvectors in a counter-clockwise way to compensate for the unwanted deviation of the symmetry plane. The symmetry plane is rotated iteratively until the changes of the Hausdorff distance between the mirrored left and right point-group become negligible. The

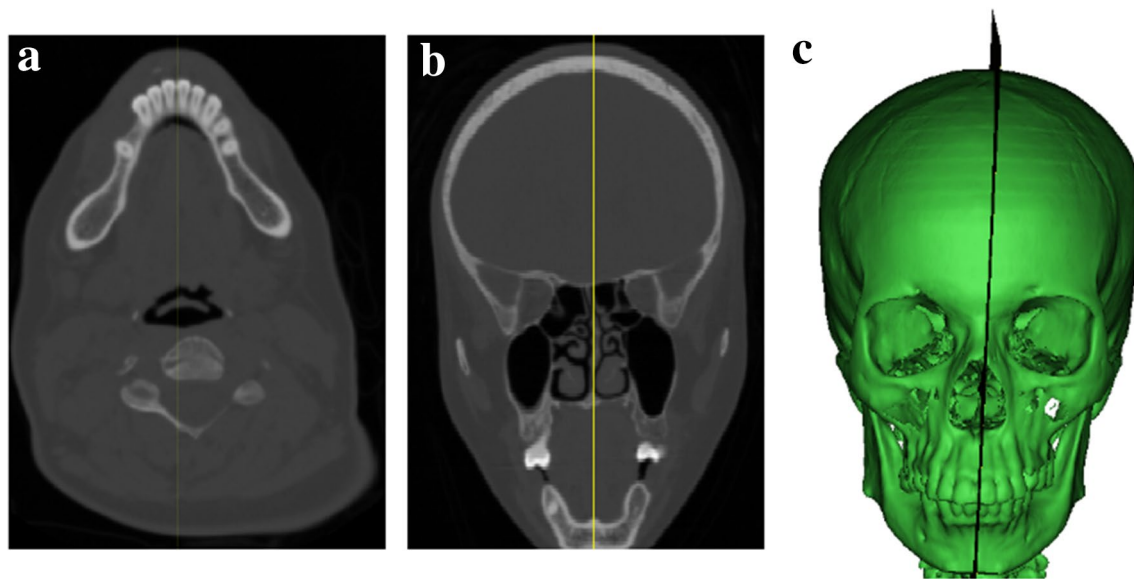


Fig. 6 Symmetry plane computed for intact data resulted from the proposed algorithm (yellow line). **a** Symmetry plane in axial view, **b** symmetry plane in coronal view, and **c** Symmetry plane in 3D view

rotational angle in each iteration refines the symmetry-plane deviation. As the noise and outliers make landmarks more asymmetric, the symmetry plane deviation and rotational angle become larger. In the early iterations, the rotational angle compensates for global deviation, while in the last iterations, local deviations are refined. The effect of the rotational angle on the symmetry plane could be adjusted with a convergence coefficient (η). Since the ICP algorithm matches two point-groups as accurately as possible, the effect of noise and outliers will be filtered robustly.

If we put aside the stated assumptions and allow the technique to apply the reverse of the translate vector on the symmetry plane, then a considerable unwanted bias occurs in the symmetry plane. Hence, the bias infiltrates the left- and right-side point-groups in the next calculations. Afterwards, in the next iteration, the ICP algorithm results deviate absolutely from the symmetry plane.

As demonstrated in the results, in just six iterations, HD decreased by around 66% in the intact skull (65% in simple unilateral midface fracture) and converged. The low number of iterations indicates that the symmetry plane could be found with a low computational load. Hausdorff

distance (HD) could be a useful error index for symmetry-plane evaluation [26]. When HD does not change significantly, the algorithm converges and must be stopped. We can trace the variation of the angle of rotation matrix vs. iteration. The results show that these changes are consistent with the HD curve.

PSR is done by the ICP algorithm with subsampling to decrease the computational load. The concept behind subsampling is to preserve the general shape [22]. The subsampling factor, r , affects the number of faces directly; consequently, the number of vertices is also changed. As the results showed, we could subsample initial input by a factor of 0.075 and the elapsed CPU time reduced 7.4 times in comparison with $r=0.2$. This is the most critical parameter for the ICP algorithm in this problem. If the reduction factor becomes smaller, then the HD is ruined and so the symmetry plane deviates.

In each iteration of the ICP algorithm, the distance between the corresponding point-pairs was updated to re-estimate the registration parameters. We ran the algorithm with kD-tree, $r=0.075$, and validated the ICP performance in the sixth iteration. The run time was reduced about 99 times in comparison with the conventional ICP algorithm.

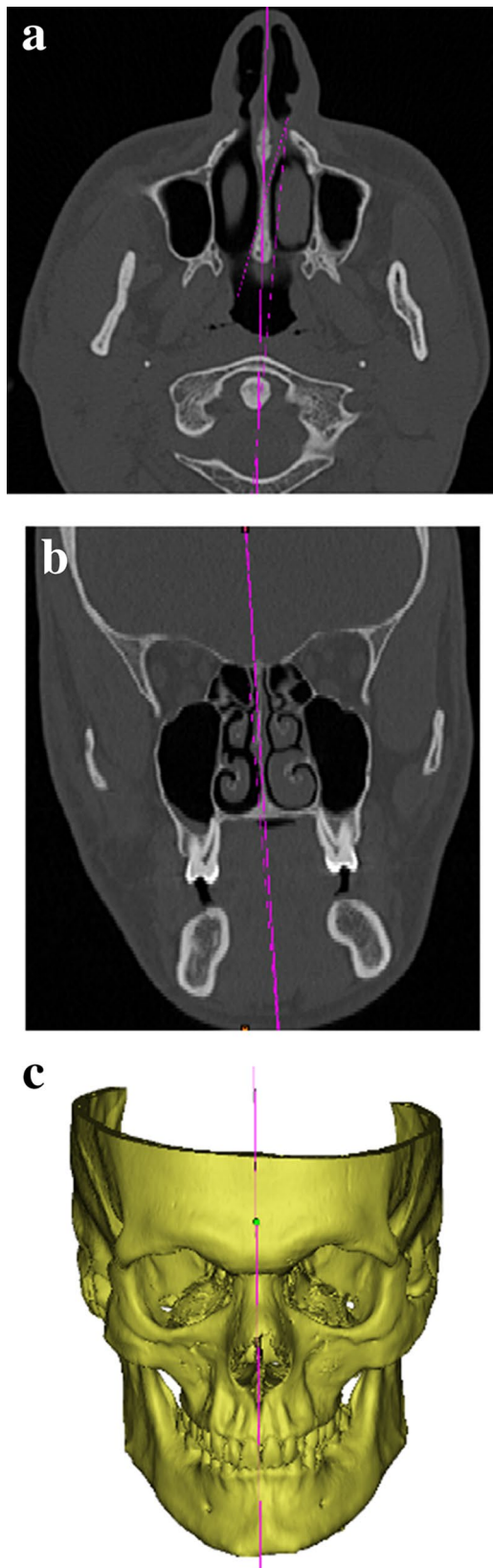


Fig. 7 Symmetry plane computed for zygomatic arch fractured data resulting from the proposed algorithm (wide purple line). **a** Symmetry plane in axial view, **b** symmetry plane in coronal view, and **c** symmetry plane in 3D view

Li et al. claim that kD-tree improves registration accuracy on Magnolia point cloud data [28], but Table 2 shows that kD-tree does not affect HD and ICP error for our datasets. This could be because of the properties of the data organisation.

As Rusinkiewicz and Levoy indicated [21] and our results confirm, each variation of the ICP algorithm could be chosen for a specific application. The results show that a mixture consists of subsampling point-sets, and the use of kD-tree for matching points improved our results significantly, in comparison with the conventional ICP algorithm.

It is notable that, in the pre-processing stage, when vertebrae exist in CT images, the head and neck may not be on the same plane. Since the head and neck have two different symmetry planes, the main symmetry plane will be missed. In such cases, we suggest eliminating neck vertebrae in pre-processing. Also, metal artefacts in the patient's teeth must be removed in the pre-processing stage.

As the results demonstrate, in a patient with a simple unilateral midface fracture, our method is robust enough to be used in order to find the best possible symmetry plane. Figure 7 demonstrates that the algorithm works well for simple unilateral fractures on the zygomatic arch. Also, it works well for the zygomatic bone, orbital rim, and ramus fractures. Indeed, the symmetry plane in fractures that do not transform data of the point-set dramatically could be found by the proposed algorithm. As Fig. 8 shows, the first rotational angle in the fractured skull may have a value approximately 60% higher than its corresponding angle in the intact skull, while in the last iterations the rotational angles became similar. This result shows the robustness of the proposed algorithm, from the ICP registration and the fact of it being iterative. In each iteration, the ICP algorithm compensates for symmetry-plane deviation and after a few iterations, the algorithm converges to an acceptable symmetry plane. Figure 9 shows that the final value of HD in intact and fractured skulls are similar and the difference is negligible.

Our method is simple and easy to implement. Implemented codes in MATLAB are available to share with researchers. It can be readily adapted for implementing with other anatomic parts, although this should be demonstrated in actual experiments. The proposed method has a promising role in correct symmetry-plane discovery and could be added in craniomaxillofacial preplanning software. Future research could be applied to use both CT and 3D facial scan images to explore a more precise symmetry plane. Furthermore, we are working on a new idea that the symmetry plane is calculated through an atlas-based algorithm to apply for patients with more complicated fractures.

Fig. 8 Rotation-angle variation derived from rotation matrix in the ICP algorithm for intact and fractured skulls

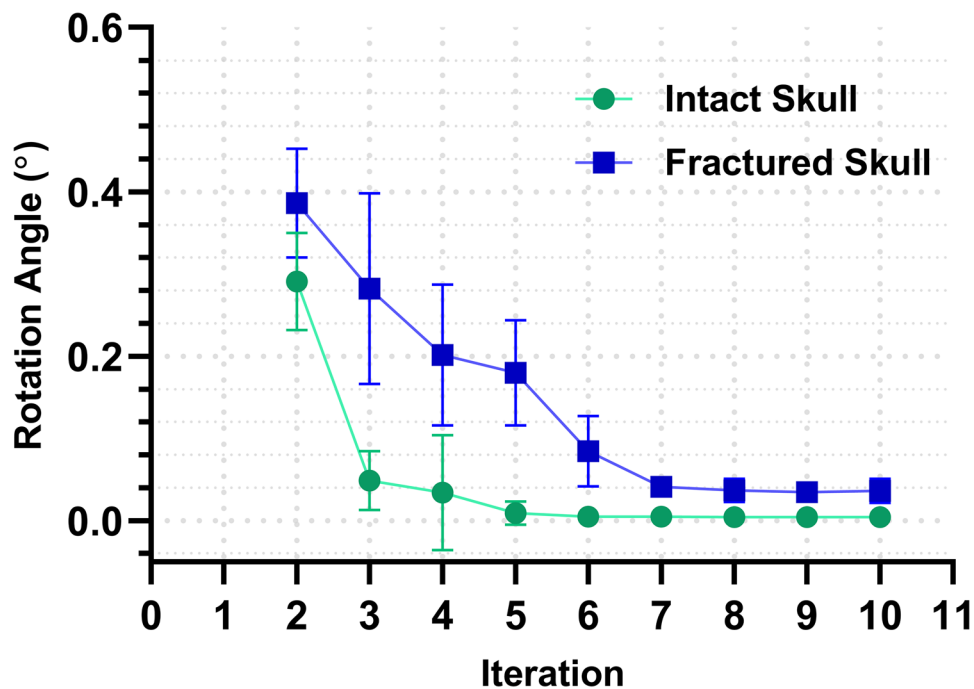
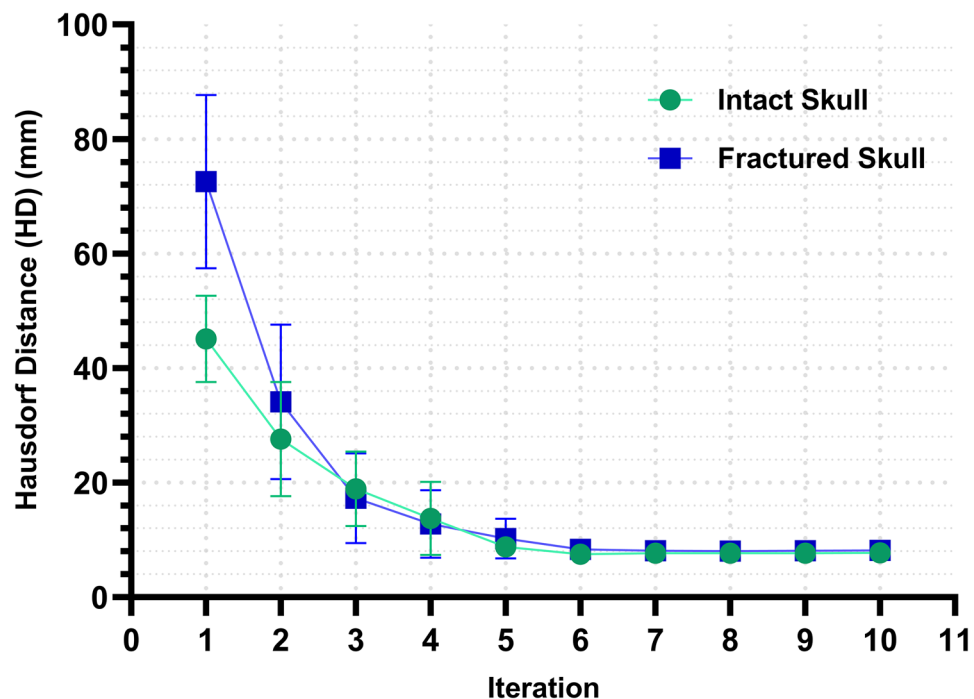


Fig. 9 Hausdorff distance values for intact and fractured skulls



Funding This study was funded by the Faculty of Medicine, Tehran University of Medical Sciences, under Grant Number 36938-30-04-96.

Compliance with ethical standards

Conflict of interest The authors declare that they have no conflict of interest.

Ethical approval All procedures performed in this study were in accordance with the ethical standards of the Tehran University of Medical Science (ethical code: IR.TUMS.MEDICINE.REC.1396.4592).


Informed consent We used archived unnamed data from Sina Hospital and Parsiss Co.

References

1. Cevidanes LHS, Alhadidi A, Paniagua B, Styner M, Ludlow J, Mol A, Turvey T, Proffit WR, Rossouw PE (2011) Three-dimensional quantification of mandibular asymmetry through cone-beam computerized tomography. *Oral Surg Oral Med Oral Pathol Oral Radiol* 111(6):757–770
2. Bockey S, Berssenbrügge P, Dirksen D, Wermker K, Klein M, Runte C (2018) Computer-aided design of facial prostheses by means of 3D-data acquisition and following symmetry analysis. *J Cranio-Maxillofac Surg* 46(8):1320–1328
3. Li J, Yuan P, Chang CM, Ho DCY, Lo YF, Shen S, Kim D, Teichgraber JF, Alfi DM, Gateno J, Xia JJ (2017) New approach to establish an object reference frame for dental arch in computer-aided surgical simulation. *Int J Oral Maxillofac Surg* 46(9):1193–1200
4. Ho JPTF, Schreurs R, Milstein DMJ, Dubois L, Maal TJJ, de Lange J, Becking AG (2016) Measuring zygomaticomaxillary complex symmetry three-dimensionally with the use of mirroring and surface based matching techniques. *J Cranio-Maxillofac Surg* 44(10):1706–1712
5. Ho JPTF, Schreurs R, Aydi S, Rezaï R, Maal TJJ, van Wijk AJ, Beenen LFM, Dubois L, Milstein DMJ, Becking AG (2017) Natural variation of the zygomaticomaxillary complex symmetry in normal individuals. *J Cranio-Maxillofac Surg* 45(12):1927–1933
6. De Momi E, Chapuis J, Pappas I, Ferrigno G, Hallermann W, Schramm A, Caversaccio M (2006) Automatic extraction of the mid-facial plane for cranio-maxillofacial surgery planning. *Int J Oral Maxillofac Surg* 35(7):636–642
7. Roumeliotis G, Willing AR, Neuert M, Ahluwalia R, Jenkyn T, Yazdani A (2015) Application of a novel semi-automatic technique for determining the bilateral symmetry plane of the facial skeleton of normal adult males. *J Craniofac Surg* 26(6):1997–2001
8. Willing RT, Roumeliotis G, Jenkyn TR, Yazdani A (2013) Development and evaluation of a semi-automatic technique for determining the bilateral symmetry plane of the facial skeleton. *Med Eng Phys* 35(12):1843–1849
9. Di Angelo L, Di Stefano P, Governi L, Marzola A, Volpe Y (2019) A robust and automatic method for the best symmetry plane detection of craniofacial skeletons. *Symmetry (Basel)* 11(2):1–13
10. Martini M, Klausning A, Messing-Jünger M, Lüchters G (2017) The self-defining axis of symmetry: a new method to determine optimal symmetry and its application and limitation in craniofacial surgery. *J Cranio-Maxillofac Surg* 45(9):1558–1565
11. AlHadidi A, Cevidanes LH, Paniagua B, Cook R, Festy F, Tyn-dall D (2014) 3D quantification of mandibular asymmetry using the SPHARM- PDM tool box. *Int J Comput Assist Radiol Surg* 7(2):265–271
12. Berlin NF, Berssenbrügge P, Runte C, Wermker K, Jung S, Kleinheinz J, Dirksen D (2014) Quantification of facial asymmetry by 2D analysis—a comparison of recent approaches. *J Cranio-Maxillofac Surg* 42(3):265–271
13. Kikinis R, Pieper SD, Vosburgh KG (2014) 3D Slicer: a platform for subject-specific image analysis, visualization, and clinical support. Intraoperative imaging and image-guided therapy. Springer, New York, pp 277–289
14. Dimitrov D (2008) Geometric applications of principal component analysis. Dissertation, University of Berlin
15. Serej ND, Ahmadian A, Kasaei S, Sadrehosseini SM, Farnia P (2016) A robust keypoint extraction and matching algorithm based on wavelet transform and information theory for point-based registration in endoscopic sinus cavity data. *Signal Image Video Process* 10(5):983–991
16. Farnia P, Ahmadian A, Khoshnevisan A, Jaberzadeh A, Serej ND, Kazerooni AF (2011) An efficient point based registration of intra-operative ultrasound images with MR images for computation of brain shift; A phantom study. *Annu Int Conf IEEE Eng Med Biol Soc* 2011:8074–8077
17. Noori SMR, Mobaraki M, Ahmadian A, Bayat M, Bahrami N (2020) Zygomatic bone registration based on a modified student's mixture model method. Piscataway, IEEE, pp 1–5
18. Farnia P, Ahmadian A, Sedighpoor M, Khoshnevisan A, Mansoori MS (2012) On the performance of improved ICP algorithms for registration of intra-ultrasound with pre-MR images; a phantom study. *Annu Int Conf IEEE Eng Med Biol Soc* 2012:4390–4393
19. Besl PJ, McKay ND (1992) Method for registration of 3-d shapes. Sensor fusion IV control paradigms and data structures, vol 1611. International Society for Optics and Photonics, Bellingham, pp 586–607
20. Chen Y, Medioni G (1992) Object modelling by registration of multiple range images. *Image Vis Comput* 10(3):145–155
21. Rusinkiewicz S, Levoy M (2001) Efficient variants of the ICP algorithm. Proceedings third international conference on 3-D digital imaging and modeling. Piscataway, IEEE, pp 145–152
22. Mathworks (2019) Parallel computing toolbox. <https://www.mathworks.com/help/matlab/ref/reducepatch.html>. Accessed 2019
23. Bentley JL (1975) Multidimensional binary search trees used for associative searching. *Commun ACM* 18(9):509
24. Sun Z, Li Z, Liu Y (2020) An improved lidar data segmentation algorithm based on euclidean clustering. In: Proceedings of the 11th international conference on modelling, identification and control, pp 1119–1130
25. Shahabi C, Kolahdouzan MR, Sharifzadeh M (2003) A road network embedding technique for K-nearest neighbor search in moving object databases. *Geoinformatica* 7(3):255–273
26. Alt H, Guibas LJ (1999) Discrete geometric shapes: matching, interpolation, and approximation. *Handb Comput Geom* 1:121–153
27. Ghadimi S, Abrishami Moghaddam H, Grebe R, Wallois F (2016) Skull segmentation and reconstruction from newborn CT images using coupled level sets. *IEEE J Biomed Heal Inform* 20(2):563–573
28. Li S, Wang J, Liang Z, Su L (2016) Tree point clouds registration using an improved icp algorithm based on kd-tree. In: 2016 IEEE International Geoscience and Remote Sensing Symposium, pp 4545–4548

Publisher's Note Springer Nature remains neutral with regard to jurisdictional claims in published maps and institutional affiliations.

Affiliations

Seyed Mohammad Reza Noori^{1,2} · Parastoo Farnia^{1,2} · Mohammad Bayat^{3,4} · Naghmeh Bahrami^{3,5} · Ali Shakourirad^{6,7} · Alireza Ahmadian^{1,2} 

✉ Alireza Ahmadian
ahmadian@tums.ac.ir

¹ Departments of Medical Physics and Biomedical Engineering, School of Medicine, Tehran University of Medical Sciences, Tehran, Iran

² Research Center for Biomedical Technologies and Robotics, Tehran University of Medical Sciences, Tehran, Iran

³ Craniomaxillofacial Research Center, Tehran University of Medical Sciences, Tehran, Iran

⁴ Oral and Maxillofacial Surgery Department, School of Dentistry, Tehran University of Medical Sciences, Tehran, Iran

⁵ Department of Tissue Engineering and Applied Cell Sciences, School of Advanced Technologies in Medicine, Tehran University of Medical Sciences, Tehran, Iran

⁶ Advanced Diagnostic and Interventional Radiology Research Center (ADIR), Sina Hospital, Tehran University of Medical Sciences, Tehran, Iran

⁷ Department of Radiology, Tehran University of Medical Sciences, Tehran, Iran